

Charged thin shells in unimodular gravity

Gabriel R. Bengochea*, Ernesto F. Eiroa†, Griselda Figueroa-Aguirre‡
Instituto de Astronomía y Física del Espacio (IAFE, CONICET-UBA),
Ciudad Universitaria, 1428, Buenos Aires, Argentina

Abstract

In this article, we construct a broad family of spacetimes with spherically symmetric thin shells in unimodular gravity. We analyze the dynamical stability of the configurations under perturbations preserving the symmetry. In particular, we consider the case of thin shells with charge surrounding vacuum, obtaining stable configurations for suitable values of the parameters. We compare our results with those corresponding to general relativity.

1 Introduction

Unimodular gravity (UG) is an alternative theory of gravity closely related to general relativity (GR), which was first considered by Einstein in 1919 [1]. In such an approach the gravitational field is described by the trace-free Einstein equations and these ones can be derived from an action, where a fixed non-dynamical 4-volume element appears, see e.g. [2–4]. The presence of this 4-volume background can be thought as something that breaks the diffeomorphism invariance of GR, turning UG into a theory invariant only under volume-preserving diffeomorphisms. An interesting feature of UG, which relevance became more popular after the work [5], is that within the framework of this theory of gravity the cosmological constant simply plays the role of an integration constant, linked to initial conditions, but which allows to decouple it from a possible vacuum quantum energy, since the latter does not gravitate in UG, see e.g. [3]. In this way, the huge discrepancy of up to 120 orders of magnitude between the observed value of the cosmological constant and the value predicted by quantum field theory (QFT) [6], known as *the cosmological constant problem*, finds an elegant solution that does not require new physics¹. But there is another feature of UG, the fact that invariance of the matter action under the restricted volume-preserving diffeomorphisms brings the possibility of a non-conservation of the energy-momentum tensor, usually represented by a *diffusion* term². Within UG this conservation becomes an extra hypothesis, which, if assumed, recovers the GR field equations. Once the conservation of the energy-momentum tensor is adopted, UG is completely equivalent to GR and consistent with all observational tests. Only when one chooses not to impose the conservation of the energy-momentum tensor it is possible to find deviations from GR. For instance, in [7] it was shown that the non-conservation of the energy-momentum tensor implies the non-geodesic motion of pointlike particles.

*e-mail: gabriel@iafe.uba.ar

†e-mail: eiroa@iafe.uba.ar

‡e-mail: gfigueroa@iafe.uba.ar

¹Of course this does not solve the mystery of why it has the *particular value* that it has today.

²Note that this same result can be obtained, without imposing such limitations, through a slightly different derivation. See Sect. 2.2 of [4]

In the last decade, interest in UG has resurged with special emphasis on the area of cosmology, see e.g. [8–22]. In particular, misconceptions regarding the notion of diffeomorphism invariance (mainly its use in UG) and the choice of gauges in the treatment of cosmological perturbations, were considered and analyzed in depth in [4]. Spherically symmetric configurations were recently explored in the context of UG [23], where the general equations for a static solution were settled out, and some examples resulting from the non-conservation of the energy-momentum tensor were shown, in the presence of an electromagnetic field as well as of a self-interacting scalar field. Proposals discussing the construction of theories of gravity leading to a non-conservation of the energy-momentum tensor can be found for instance in [24]. On the other hand, in [25] the authors analyze the “fate” of energy conservation within the various viable paths to address conceptual problems, when the standard quantum setting and the semiclassical gravity program are addressed, concluding that we will probably have to accept the fact that, neither Einstein equations nor conservation laws hold in the world we actually experience. It is also interesting to mention that, within the context of QFT on curved spacetimes, considerations related to the issue of renormalization of the energy-momentum tensor in the semiclassical gravity framework [26] also seem to suggest a preference for UG. Some theoretical proposals coming from some quantum gravity approaches suggest that, at the Planck scale, a more fundamental physics is expected to be discrete. For this approach to be compatible with Lorentz symmetry³, such a discreteness would have to be realized by the existence of some kind of 4-volume elementary building blocks, which would produce a background 4-volume structure where only invariance under volume-preserving diffeomorphisms would be present, thus allowing UG to be considered as a natural effective description of gravity at low energies [28]. Also, Planck-scale discreteness could play a role in black hole physics [29], and in a possible resolution of the information paradox associated with black holes [30, 31]. For a recent discussion of these topics, see e.g. [32]. On the other hand, since the detection of the accelerated expansion of the universe, extensive studies are being conducted to understand whether this acceleration is due to a cosmological constant, a dynamical dark energy, or a modification of the theory of gravity. The use of UG, with the perspective that the energy-momentum non-conservation is due to a fundamental granularity of the spacetime at Planckian scales, was implemented to search for answers about the nature of dark energy, the H_0 tension, and the current value of the cosmological constant in recent works [12–14], as well as to find a possible alternative for the inflationary phase (without an inflaton field) of the early universe [20, 33].

Thin shells of matter appear as idealized useful models in many physical contexts. In GR, the Darmois–Israel [34, 35] junction conditions provide the tools for the construction of a new spacetime by joining two different geometries across a hypersurface. The formalism allows to analyze the characteristics and dynamics of thin shells, relating the energy-momentum tensor at the matching hypersurface with the geometries at both sides of it. The formalism has been broadly applied in many situations because of its simplicity and flexibility; the stability analysis is easy to perform in case of highly symmetric configurations, for perturbations preserving the symmetry. Many researchers have adopted this formalism to model vacuum bubbles and thin layers around black holes [36–41], fluid spheres supported by thin shells [42], wormholes [43–50], and gravastars [51–54]. There are also studies in which the junction conditions are used to build wormholes and thin shells of matter in N dimensions [55–58]. The junction conditions have been obtained in some theories of modified gravity. Different physical scenarios have been considered within $F(R)$ gravity in four dimensions by using this technique [59–63], and also in lower [64, 65] and in higher [66] dimensionality. Spacetimes with thin shells were also analyzed within Palatini $F(R)$ gravity [67], in $F(R, T)$ gravity [68], and in Brans-Dicke theory [69, 70].

³Issues related to compatibility with Lorentz invariance when a discrete spacetime is considered, can be found in, e.g. [27].

In this article, we study thin shells within UG with the help of the corresponding junction conditions introduced in [3]. We start in Sec. 2 with a review of the main aspects of the theory and the recently found spherically symmetric black hole solutions in the presence of the electromagnetic field [23]. In Sec. 3, we construct spherically symmetric thin shells within UG and we obtain the condition for stability under radial perturbations. In Sec. 4, we provide examples of charged thin shells surrounding vacuum (bubbles), with flat, de Sitter, and anti-de Sitter asymptotics. Finally, in Sec. 5, we present the conclusions of this work. Throughout the paper, we use the $(-, +, +, +)$ signature for the spacetime metric and we adopt units such that $c = G = 1$.

2 Black holes in unimodular gravity

Let us start this section with the field equations of UG, which can be obtained from a variational principle, requiring the extremization $\delta S = 0$, with the action written as [4]⁴,

$$S[g^{ab}, \Psi_M; \Lambda] = \frac{1}{2\kappa} \int \left[R\epsilon_{abcd}^{(g)} - 2\Lambda(\epsilon_{abcd}^{(g)} - \varepsilon_{abcd}) \right] + S_M[g^{ab}, \Psi_M], \quad (1)$$

where we define $\kappa \equiv 8\pi$, R is the Ricci scalar, and ε_{abcd} and $\epsilon_{abcd}^{(g)}$ are a fiduciary 4-volume element (given by the theory) and a 4-volume element associated to the metric g_{ab} , respectively. The scalar $\Lambda(x)$ is a Lagrange multiplier function, and S_M is the action of the matter fields generically represented by Ψ_M . Variations of (1) with respect to dynamical variables g^{ab} , Λ and Ψ_M lead to

$$R_{ab} - \frac{R}{2}g_{ab} + \Lambda(x)g_{ab} = \kappa T_{ab}, \quad (2)$$

$$\epsilon_{abcd}^{(g)} = \varepsilon_{abcd}, \quad (3)$$

$$\frac{\delta S^M}{\delta \Psi_M} = 0. \quad (4)$$

On the right-side of Eqs. (2) the energy-momentum tensor appears, which is defined as

$$T_{ab} \equiv \frac{-2}{\sqrt{-g}} \frac{\delta S_M}{\delta g^{ab}}. \quad (5)$$

Note that in the last expression g is the determinant of the components of the metric tensor, $g_{\mu\nu}$, in a specific coordinate basis. On the other hand, Eq. (4) yields the equation of motion of the matter fields (i.e. a Klein-Gordon type equation).

At this point, the trace of Eq. (2) allows us to write Λ as

$$\Lambda = \frac{\kappa T + R}{4}, \quad (6)$$

where $T = g^{ab}T_{ab}$ is the trace of the energy-momentum tensor. Next, by substituting the former expression into Eq. (2), it leads to the trace-free part of Einstein field equations, namely

$$R_{ab} - \frac{1}{4}g_{ab}R = \kappa \left(T_{ab} - \frac{1}{4}g_{ab}T \right), \quad (7)$$

⁴To avoid some of the misconceptions mentioned in [4], we will first use indexes following Wald's convention and notation for the geometrical objects [71], which makes a distinction between index notation and component notation. Then, we will denote components of a tensor in a given basis by using Greek indices.

which are the UG equations for the gravitational field. Note that anything behaving like a cosmological constant or vacuum energy does not gravitate, since it automatically satisfies that the right-hand side of (7) is zero.

As we mentioned in the Introduction, one of the interesting features of UG that allows departures from GR is the possibility of the non-conservation of the energy-momentum tensor; indeed, Eq. (2) lets $\nabla^a T_{ab} \neq 0$. This can be demonstrated rigorously in alternative ways, noting that the important point is that, as the theory is presented through action (1), UG has a non-dynamical element that can lead to the non-conservation of T_{ab} . In UG, g^{ab} , Λ and Ψ_M are dynamical variables, while the 4-volume element ε_{abcd} is fixed and non-dynamical. One can choose to consider the variation of the action (1) involving all the geometric objects, that is, applying diffeomorphisms on both dynamical and non-dynamical variables or, alternatively, although the action (1) (by construction) is invariant under generic one-parameter family of diffeomorphism, one may restrict the consideration to the volume preserving diffeomorphisms when performing the variation of the matter action S_M . Both paths lead to [4]

$$\nabla^a (T_{ab} - g_{ab} \mathcal{D}) = 0, \quad (8)$$

where $\mathcal{D}(x)$ is an arbitrary scalar field (i.e. the *diffusion term*) that encapsulates the non-conservation possibility.

From Eq. (8), applying the covariant derivative ∇^a to both sides of Eq. (2) and using the Bianchi's identities $\nabla^a [R_{ab} - \frac{1}{2} g_{ab} R] = 0$ one obtain that

$$\Lambda(x) = \Lambda_0 + \kappa \mathcal{D}(x), \quad (9)$$

where Λ_0 is simply a constant of integration, fixed by initial data. Note that, the case $\mathcal{D}(x) = \text{constant}$ leads to the standard conservation law for T_{ab} . In the present work, we will be analyzing some particular forms for $\Lambda(x)$ motivated by the recent results of [23].

In the article [23], spherically symmetric solutions of the unimodular field equations were found, with a line element having the form

$$ds^2 = -A(r)dt^2 + A^{-1}(r)dr^2 + r^2(d\theta^2 + \sin^2 \theta d\varphi^2), \quad (10)$$

where the usual Schwarzschild (t, r, θ, φ) coordinates are used. Following [23], we adopt two different functions $\Lambda(r)$, corresponding to two distinct behaviors both asymptotically and in the center ($r = 0$), and we include a radial electric field $E(r)$ associated with a charge Q .

Case A

With the choice of a power law

$$\Lambda(r) = \Lambda_0 + \Lambda_1 r^p, \quad (11)$$

where Λ_1 is a constant, the field equations have the solution [23] determined by

- $p \neq -4, -3$:

$$A(r) = 1 - \frac{2M}{r} + \frac{Q^2}{r^2} - \frac{\Lambda_0}{3} r^2 - \frac{4\Lambda_1}{(p+3)(p+4)} r^{p+2}, \quad (12)$$

$$E^2(r) = \frac{Q^2}{r^4} - \frac{p}{p+4} \Lambda_1 r^p; \quad (13)$$

- $p = -4$:

$$A(r) = 1 - \frac{2M}{r} + \frac{Q^2}{r^2} - \frac{\Lambda_0 r^2}{3} + \frac{4\Lambda_1}{r^2} (1 + \ln r), \quad (14)$$

$$E^2(r) = \frac{Q^2}{r^4} - \frac{4\Lambda_1}{r^4} \ln r; \quad (15)$$

- $p = -3$:

$$A(r) = 1 - \frac{2M}{r} + \frac{Q^2}{r^2} - \frac{\Lambda_0 r^2}{3} + \frac{4\Lambda_1}{r} (1 - \ln r), \quad (16)$$

with the squared electric field given by Eq. (13).

It is important to note that:

- $p = -4$: this case is clearly pathological since the electric field becomes imaginary near $r = 0$ when $\Lambda_1 > 0$, or for large r if $\Lambda_1 < 0$.
- $p = 0$: this case reduces to the GR solution (Reissner-Nordström with a cosmological constant) after the redefinition $\Lambda_0 \rightarrow \Lambda_0 + \Lambda_1$.
- $p = -2$: in this particular case, the metric function can be rearranged in the form

$$A(r) = 1 - 2\Lambda_1 - \frac{2M}{r} + \frac{Q^2}{r^2} - \frac{\Lambda_0 r^2}{3},$$

so, after an appropriate change of coordinates, the spacetime presents an angular deficit if $\Lambda_1 > 0$ or an angular surplus when $\Lambda_1 < 0$.

Case B

For the second choice

$$\Lambda(r) = \Lambda_0 + \frac{\Lambda_1}{(r^2 + b^2)^2}, \quad (17)$$

where b is a constant, the field equations have the solution [23] given by

$$A(r) = 1 - \frac{2M}{r} + \frac{Q^2}{r^2} - \frac{\Lambda_0}{3} r^2 - \frac{2\Lambda_1}{r^2} \left[\frac{r}{b} \arctan\left(\frac{r}{b}\right) - \ln\left(1 + \frac{r^2}{b^2}\right) \right], \quad (18)$$

$$E^2(r) = \frac{Q^2}{r^4} + \frac{\Lambda_1}{r^4} \left[\frac{b^2(3b^2 + 4r^2)}{(b^2 + r^2)^2} + 2 \ln\left(1 + \frac{r^2}{b^2}\right) \right]. \quad (19)$$

Note that no change of sign in $E^2(r)$ can be assured by taking $\Lambda_1 > 0$.

In both cases, for small enough values of charge, the spacetime corresponds to a black hole with a singularity at the center; as the charge grows beyond the extremal value, the event horizon vanishes and the singularity is naked [23]. In particular, when $\Lambda_1 = 0$ both solutions reduce to the Reissner-Nordström with a cosmological constant Λ_0 spacetime of GR.

3 Spherical shells: construction and stability

In this section we study spherically symmetric thin shells, where a matter layer appears as the result of cutting and pasting two manifolds at a surface in order to construct a new manifold. We start from the geometries

$$ds_{1,2}^2 = -A_{1,2}(r_{1,2})dt_{1,2}^2 + A_{1,2}^{-1}(r_{1,2})dr_{1,2}^2 + r_{1,2}^2(d\theta^2 + \sin^2\theta d\varphi^2), \quad (20)$$

and we take the spherical surface Σ such as $r_{1,2} = a$. We define \mathcal{M}_1 as the set of points with radial coordinate $r_1 \leq a$ and \mathcal{M}_2 the one with $r_2 \geq a$. We join them at Σ , so the resulting manifold \mathcal{M} is the union of the inner part \mathcal{M}_1 and the outer part \mathcal{M}_2 . With a suitable identification, we can

introduce a global radial coordinate r in \mathcal{M} , with the surface Σ located at $r = a$. For the study of the stability of our construction, we let the radius a to be a function the proper time τ measured by an observer at the joining surface. The line element is continuous across Σ as the time coordinates in each side are chosen to satisfy $d\tau^2 = A_1(a)^2 (A_1(a) + \dot{a}^2)^{-1} dt_1^2 = A_2(a)^2 (A_2(a) + \dot{a}^2)^{-1} dt_2^2$, where the dot stands for $d/d\tau$. The induced metric on Σ then reads

$$ds_\Sigma^2 = -d\tau^2 + a^2(\tau)(d\theta^2 + \sin^2\theta d\varphi^2). \quad (21)$$

We denote the coordinates of the embedding by $X_{1,2}^\mu = (t_{1,2}, r, \theta, \varphi)$ and the coordinates at the surface Σ by $\xi^i = (\tau, \theta, \varphi)$. The relation between the geometry and the matter on this surface in UG takes the form [3]

$$- \left[K_{\mu\nu} - K \left(h_{\mu\nu} - \frac{1}{2} g_{\mu\nu} \right) \right] = 8\pi \left(S_{\mu\nu} - \frac{1}{4} S g_{\mu\nu} \right), \quad (22)$$

where $h_{\mu\nu}$ is the induced metric on Σ , $K_{\mu\nu}$ is the extrinsic curvature, K is its trace, and $S_{\mu\nu}$ is the surface energy-momentum tensor; the brackets $[\Upsilon] = \Upsilon^2|_\Sigma - \Upsilon^1|_\Sigma$ denote the jump of Υ across the surface. The geometry is continuous across Σ , i.e. $[h_{\mu\nu}] = 0$, as demanded by the junction formalism. If $[K_{ij}] = 0$ we speak of Σ as a boundary surface and if $[K_{ij}] \neq 0$ we say that there is a thin shell of matter at Σ . The general form of the components of K_{ij} at each side of Σ are given by

$$K_{ij}^{1,2} = -n_\gamma^{1,2} \left(\frac{\partial^2 X_{1,2}^\gamma}{\partial \xi^i \partial \xi^j} + \Gamma_{\alpha\beta}^\gamma \frac{\partial X_{1,2}^\alpha}{\partial \xi^i} \frac{\partial X_{1,2}^\beta}{\partial \xi^j} \right) \Big|_\Sigma, \quad (23)$$

where $n_\gamma^{1,2}$ are unit normals ($n^\gamma n_\gamma = 1$) to Σ . With the definition $\mathcal{H}(r) = r - a(\tau) = 0$, they take the form

$$n_\gamma^{1,2} = \left| g^{\alpha\beta} \frac{\partial \mathcal{H}}{\partial X_{1,2}^\alpha} \frac{\partial \mathcal{H}}{\partial X_{1,2}^\beta} \right|^{-1/2} \frac{\partial \mathcal{H}}{\partial X_{1,2}^\gamma}, \quad (24)$$

where the unit normals at both sides of Σ are oriented outwards from the origin. In this way, the normal to Σ is unique and points from region 1 to region 2 as required by the sign convention used in Eq. (22). We adopt the orthonormal basis $\{e_{\hat{\tau}} = e_\tau, e_{\hat{\theta}} = a^{-1}e_\theta, e_{\hat{\varphi}} = (a \sin\theta)^{-1}e_\varphi\}$ at the shell. Within this frame, for the metric (20), the first fundamental form reads $h_{i\hat{j}}^{1,2} = \text{diag}(-1, 1, 1)$, the unit normal is

$$n_\gamma^{1,2} = \left(-\dot{a}, \frac{\sqrt{A_{1,2}(a) + \dot{a}^2}}{A_{1,2}(a)}, 0, 0 \right), \quad (25)$$

and the second fundamental form has the only non-null components

$$K_{\hat{\theta}\hat{\theta}}^{1,2} = K_{\hat{\varphi}\hat{\varphi}}^{1,2} = \frac{1}{a} \sqrt{A_{1,2}(a) + \dot{a}^2} \quad (26)$$

and

$$K_{\hat{\tau}\hat{\tau}}^{1,2} = -\frac{A'_{1,2}(a) + 2\ddot{a}}{2\sqrt{A_{1,2}(a) + \dot{a}^2}}, \quad (27)$$

where the prime stands for d/dr . We consider a conservative perfect fluid for the surface energy-momentum tensor, which in the orthonormal basis has the form $S_{i\hat{j}} = \text{diag}(\sigma, p, p)$, with σ the surface energy density and p the isotropic transverse pressure. From Eq. (22), with the help of Eqs. (26) and (27), we obtain

$$\sigma = -\frac{1}{4\pi a} \left(\sqrt{A_2(a) + \dot{a}^2} - \sqrt{A_1(a) + \dot{a}^2} \right) \quad (28)$$

and

$$p = -\frac{\sigma}{2} + \frac{1}{16\pi} \left(\frac{2\ddot{a} + A_2'(a)}{\sqrt{A_2(a) + \dot{a}^2}} - \frac{2\ddot{a} + A_1'(a)}{\sqrt{A_1(a) + \dot{a}^2}} \right). \quad (29)$$

The expressions of σ and p have the same form as in GR, the reason seems to be that we have adopted a conservative surface energy-momentum tensor for the perfect fluid at the shell. These two equations above, or any of them plus the equation

$$\frac{d(a^2\sigma)}{d\tau} + p\frac{da^2}{d\tau} = 0, \quad (30)$$

determine the evolution of the shell radius as a function of τ . Considering that $\mathcal{A} = 4\pi a^2$ is the area of Σ , the first term can be understood as the change of the internal energy $\epsilon = \sigma\mathcal{A}$, while the second one represents the work done by the pressure, so this equation provides an energy balance on the shell. With the help of a given equation of state $p = p(\sigma)$, we can formally integrate Eq. (30) to give $\sigma = \sigma(a)$. For the analysis of the mechanical stability of a static thin shell with radius a_0 , we now consider small perturbations preserving the symmetry. In this static case, the energy density and the pressure are given by

$$\sigma_0 = -\frac{1}{4\pi a_0} \left(\sqrt{A_2(a_0)} - \sqrt{A_1(a_0)} \right) \quad (31)$$

and

$$p_0 = -\frac{\sigma_0}{2} + \frac{1}{16\pi} \left(\frac{A_2'(a_0)}{\sqrt{A_2(a_0)}} - \frac{A_1'(a_0)}{\sqrt{A_1(a_0)}} \right). \quad (32)$$

After some algebraic manipulations, from Eq. (28) we obtain

$$\dot{a}^2 + V(a) = 0, \quad (33)$$

where

$$V(a) = \frac{A_1(a) + A_2(a)}{2} - (2\pi a\sigma(a))^2 - \left(\frac{A_1(a) - A_2(a)}{8\pi a\sigma(a)} \right)^2 \quad (34)$$

is commonly interpreted as a potential, given the analogy between Eq. (33) and the energy of a point particle with only one degree of freedom. This potential can be expanded around the static solution, to give

$$V(a) = V(a_0) + V'(a_0)(a - a_0) + \frac{V''(a_0)}{2}(a - a_0)^2 + \mathcal{O}(a - a_0)^3. \quad (35)$$

It is straightforward to see that $V(a_0) = 0$. The first derivative of the potential takes the form

$$\begin{aligned} V'(a) &= \frac{A_1'(a) + A_2'(a)}{2} - \frac{(A_1(a) - A_2(a))(A_1'(a) - A_2'(a))}{32\pi^2 a^2 \sigma(a)^2} \\ &\quad + (\sigma(a) + a\sigma'(a)) \left(\frac{(A_1(a) - A_2(a))^2}{32\pi^2 a^3 \sigma(a)^3} - 8\pi^2 a\sigma(a) \right); \end{aligned} \quad (36)$$

from Eq. (30) we find that $a\sigma'(a) = -2(\sigma(a) + p(a))$, then

$$\begin{aligned} V'(a) &= \frac{A_1'(a) + A_2'(a)}{2} - \frac{(A_1(a) - A_2(a))(A_1'(a) - A_2'(a))}{32\pi^2 a^2 \sigma(a)^2} \\ &\quad - (\sigma(a) + 2p(a)) \left(\frac{(A_1(a) - A_2(a))^2}{32\pi^2 a^3 \sigma(a)^3} - 8\pi^2 a\sigma(a) \right). \end{aligned} \quad (37)$$

After some algebra one can verify that $V'(a_0) = 0$. The second derivative of the potential reads

$$\begin{aligned}
V''(a) = & \frac{A_1''(a) + A_2''(a)}{2} - \frac{(A_1(a) - A_2(a))(A_1''(a) - A_2''(a))}{32\pi^2 a^2 \sigma(a)^2} \\
& - \frac{(A_1'(a) - A_2'(a))^2}{32\pi^2 a^2 \sigma(a)^2} + (a\sigma'(a) - 2p(a)) \frac{(A_1(a) - A_2(a))(A_1'(a) - A_2'(a))}{16\pi^2 a^3 \sigma(a)^3} \\
& + (\sigma(a)(-2ap'(a) + 6p(a) + 3\sigma(a)) + 2a(3p(a) + \sigma(a))\sigma'(a)) \frac{(A_1(a) - A_2(a))^2}{32\pi^2 a^4 \sigma(a)^4} \\
& + 8\pi^2 (\sigma(a)(2ap'(a) + 2p(a) + \sigma(a)) + 2a(p(a) + \sigma(a))\sigma'(a)). \tag{38}
\end{aligned}$$

We adopt at the shell the linearized equation of state

$$p - p_0 = \eta(\sigma - \sigma_0) + \mathcal{O}(\sigma - \sigma_0)^2 \tag{39}$$

where η is a parameter that can be interpreted as the fluid squared velocity of sound if $0 \leq \eta < 1$. Using again that $a\sigma'(a) = -2(\sigma(a) + p(a))$, the second derivative of the potential evaluated at a_0 reads

$$\begin{aligned}
V''(a_0) = & \frac{A_1''(a_0) + A_2''(a_0)}{2} - \frac{(A_2(a_0) - A_1(a_0))(A_2''(a_0) - A_1''(a_0))}{32\pi^2 a_0^2 \sigma_0^2} \\
& - \frac{(A_1'(a_0) - A_2'(a_0))^2}{32\pi^2 a_0^2 \sigma_0^2} - (\sigma_0 + 2p_0) \frac{(A_1(a_0) - A_2(a_0))(A_1'(a_0) - A_2'(a_0))}{8\pi^2 a_0^3 \sigma_0^3} \\
& - (2(5 - 2\eta)p_0\sigma_0 + 12p_0^2 + (1 - 4\eta)\sigma_0^2) \frac{(A_1(a_0) - A_2(a_0))^2}{32\pi^2 a_0^4 \sigma_0^4} \\
& - 8\pi^2 (2(2\eta + 3)p_0\sigma_0 + 4p_0^2 + (4\eta + 3)\sigma_0^2), \tag{40}
\end{aligned}$$

where σ_0 and p_0 are given by Eqs. (31) and (32), respectively. By replacing the expressions of σ_0 and p_0 , we can rewrite the second derivative of the potential in the form

$$\begin{aligned}
V''(a_0) = & -\frac{\sqrt{A_2(a_0)}A_1''(a_0) - \sqrt{A_1(a_0)}A_2''(a_0)}{\sqrt{A_1(a_0)} - \sqrt{A_2(a_0)}} + \frac{A_2(a_0)^{3/2}A_1'(a_0)^2 - A_1(a_0)^{3/2}A_2'(a_0)^2}{2A_1(a_0)A_2(a_0) \left(\sqrt{A_1(a_0)} - \sqrt{A_2(a_0)}\right)} \\
& - (2\eta + 1) \frac{\sqrt{A_2(a_0)}(a_0 A_1'(a_0) - 2A_1(a_0)) - \sqrt{A_1(a_0)}(a_0 A_2'(a_0) - 2A_2(a_0))}{a_0^2 \left(\sqrt{A_1(a_0)} - \sqrt{A_2(a_0)}\right)}. \tag{41}
\end{aligned}$$

The configuration is stable under radial perturbations when $V''(a_0) > 0$.

4 Charged shells surrounding vacuum

Let us introduce a concrete example. For the inner zone we adopt a Minkowski geometry, that is $A_1(r) = 1$, and for the outer region the UG spacetime introduced in Sec. 2, determined by the metric function $A_2(r)$, given by Eqs. (12), (14), or (16) in the case A and by Eq. (18) in the case B. The possible horizons are determined by the real and positive zeros of the function $A_2(r)$. In our construction, the radius a_0 of the thin shell is taken larger than the radius r_h of the event horizon but smaller than the radius r_c of cosmological horizon of the original manifold corresponding to the outer part, if any of them exist. In this way, we obtain a vacuum region surrounded by a charged thin shell, i.e. a charged bubble, without singularities and event horizons. In some scenarios, a

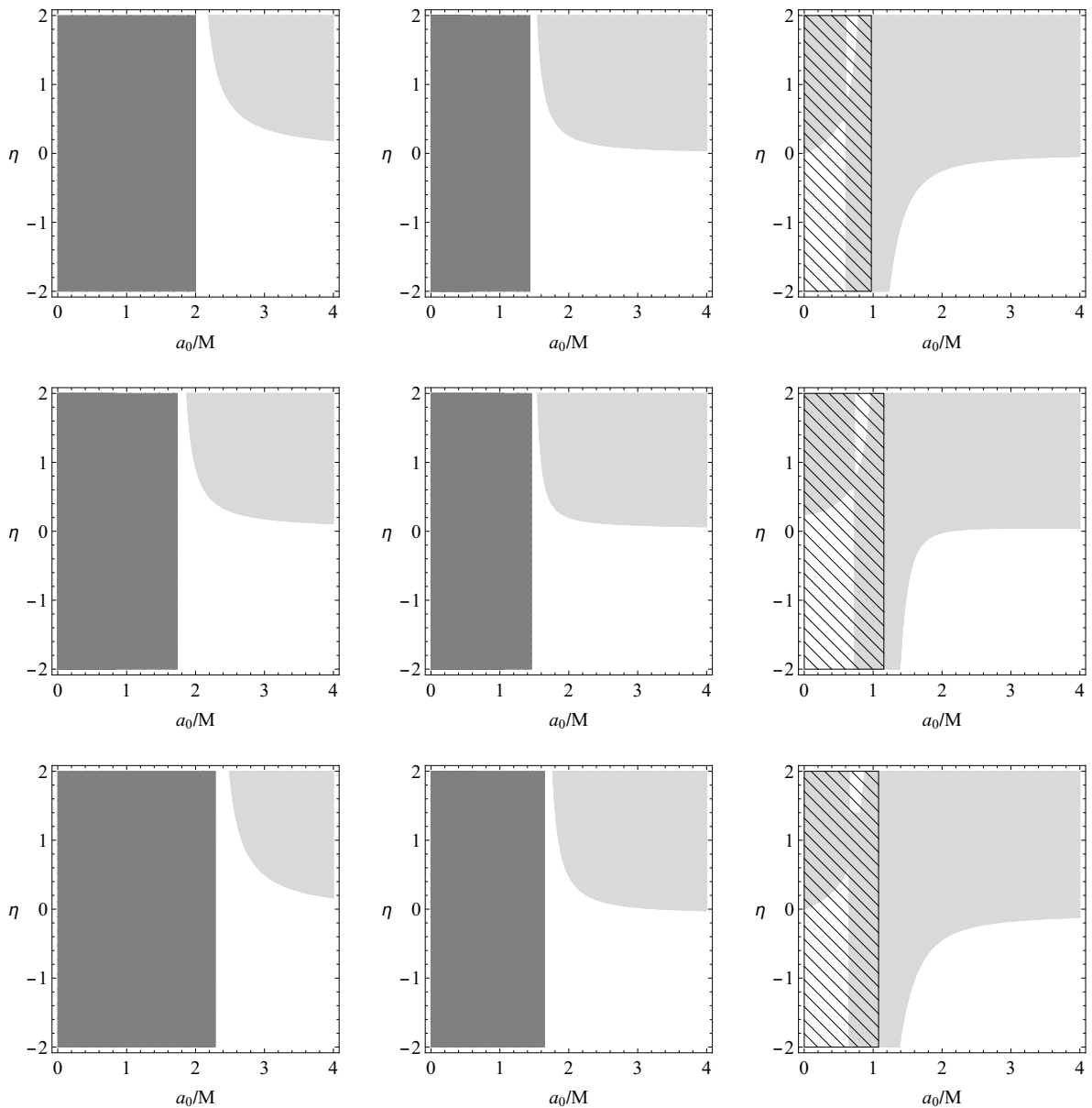


Figure 1: Regions of stability in the $(a/M, \eta)$ plane for $\Lambda_0 M^2 = 0$. The top row displays the results corresponding to GR ($\Lambda_1 = 0$), for which $Q_c/M = 1$; the center row to the case A with $p = -5$ and $\Lambda_1 M^{p+2} = -0.4$, for which $Q_c/M = 0.54$; and the bottom row to the case B with $b/M = 1$ and $\Lambda_1/M^2 = 0.4$, for which $Q_c/M = 1.04$. The left column shows the plots with $Q = 0$, the center column with $|Q| = 0.9Q_c$, and the right column with $|Q| = 1.1Q_c$. Configurations in the light gray zone are stable, the dashed area represents thin shells not satisfying WEC, and the dark gray region is non-physical.

cosmological horizon is present, located outside the shell. The energy density and the pressure are given by Eqs. (31) and (32), respectively. We distinguish between the configurations where the matter at Σ satisfies the weak energy condition (WEC), i.e. $\sigma_0 \geq 0$ and $\sigma_0 + p_0 \geq 0$ for our conservative perfect fluid, from those that do not. From Eq. (41) we can determine the stability

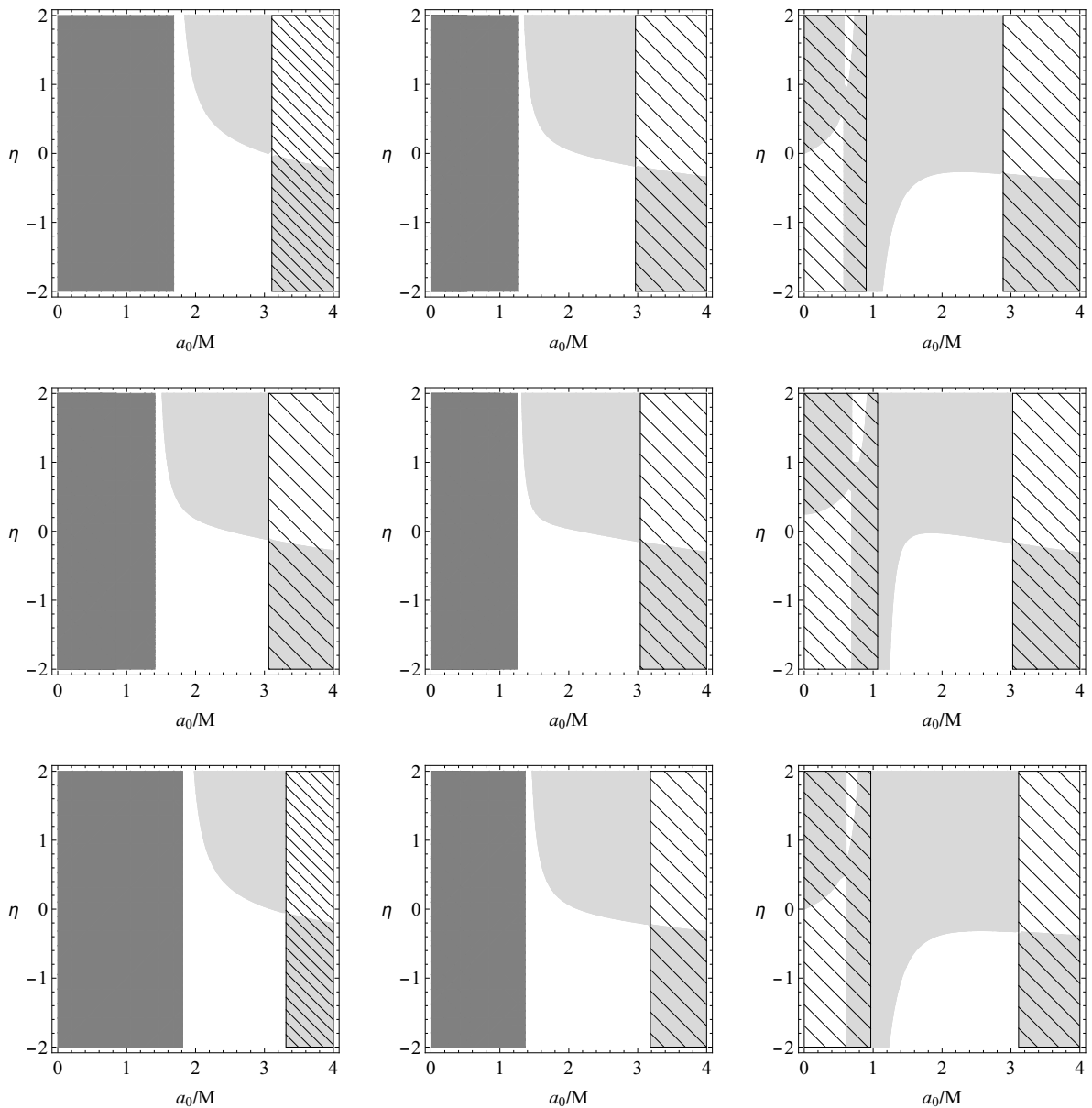


Figure 2: Regions of stability in the $(a/M, \eta)$ plane for $\Lambda_0 M^2 = -0.2$. The top row displays the results corresponding to GR ($\Lambda_1 = 0$), for which $Q_c/M = 0.97$; the center row to the case A with $p = -5$ and $\Lambda_1 M^{p+2} = -0.4$, for which $Q_c/M = 0.40$; and the bottom row to case B with $b/M = 1$ and $\Lambda_1/M^2 = 0.4$, for which $Q_c/M = 1.00$. The left column shows the plots with $Q = 0$, the center column with $|Q| = 0.9Q_c$, and the right column with $|Q| = 1.1Q_c$. Configurations in the light gray zone are stable, the dashed area represents thin shells not satisfying WEC, and the dark gray region is non-physical.

of the static configurations by using that $V''(a_0) > 0$ corresponds to the stable ones.

For the case A, we consider in our analysis the exponent $p = -5$ in Eq. (12), as a representative example. There exists a critical value of charge Q_c , where the number of horizons changes, that plays an important role. For $\Lambda_0 > 0$ the metric always has the cosmological horizon; in addition,

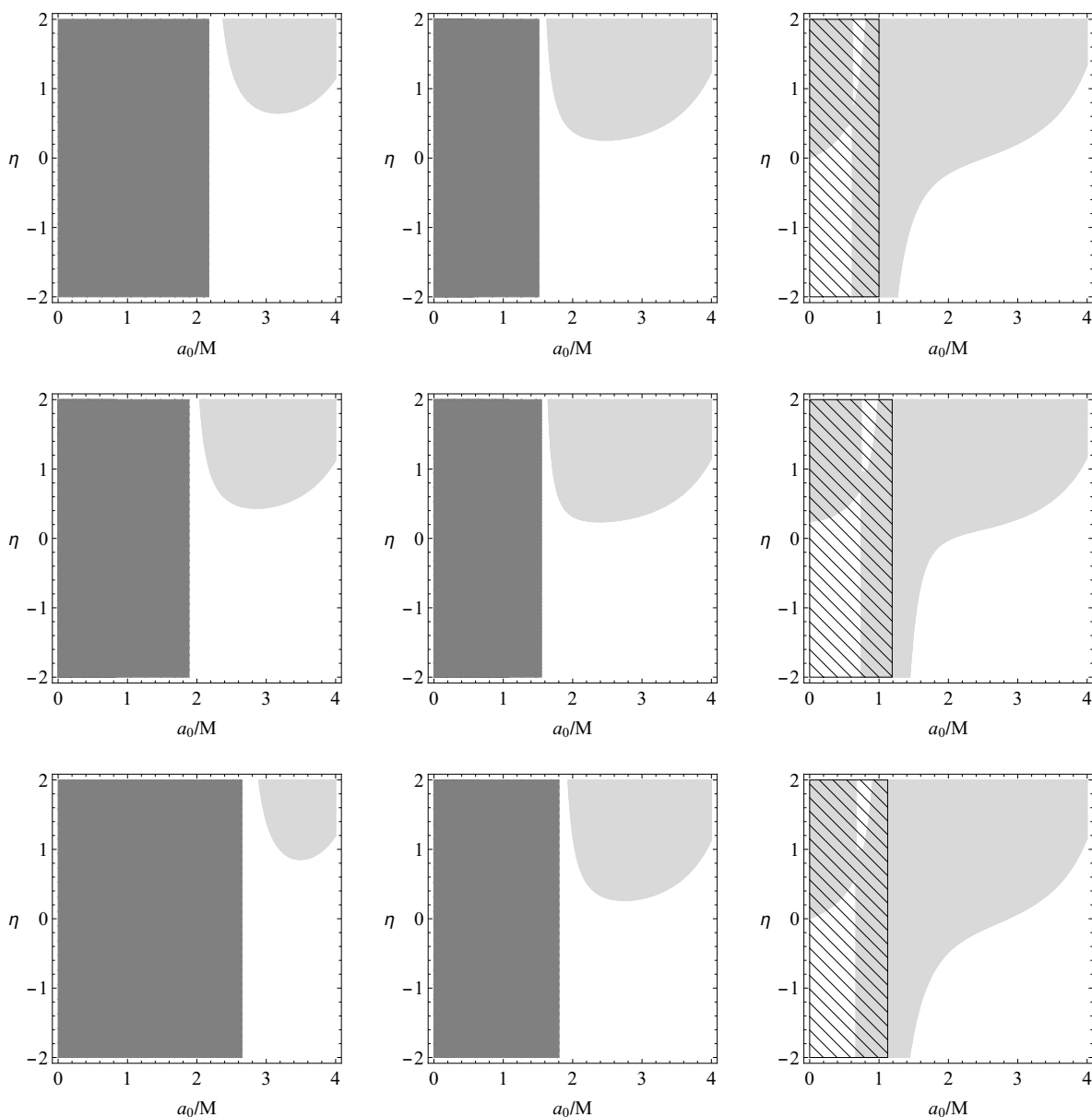


Figure 3: Regions of stability in the $(a/M, \eta)$ plane for $\Lambda_0 M^2 = 0.05$. The top row displays the results corresponding to GR ($\Lambda_1 = 0$), for which $Q_c/M = 1.00$; the center row to the case A with $p = -5$ and $\Lambda_1 M^{p+2} = -0.4$, for which $Q_c/M = 0.58$; and the bottom row to case B with $b/M = 1$ and $\Lambda_1/M^2 = 0.4$, for which $Q_c/M = 1.05$. The left column shows the plots with $Q = 0$, the center column with $|Q| = 0.9Q_c$, and the right column with $|Q| = 1.1Q_c$. The cosmological horizons are located at the radius (from left to right) $r_c/M = 6.42, 6.54, 6.59$ (top row), $r_c/M = 6.44, 6.48, 6.50$ (center row), and $r_c/M = 5.68, 5.89, 5.98$ (bottom row). Configurations in the light gray zone are stable, the dashed area represents thin shells not satisfying WEC, and the dark gray region is non-physical.

if $Q = 0$ there is an event horizon, for $0 < |Q| < Q_c$ it has the inner and the event horizons, and when $|Q| = Q_c$ they fuse into one to finally disappear if $|Q| > Q_c$, having a naked singularity at the

origin. For $\Lambda_0 < 0$, if $0 < |Q| < Q_c$ the inner and the event horizons are present, when $|Q| = Q_c$ they merge, and finally if $|Q| > Q_c$ there is a naked singularity and there are no horizons. As mentioned above, when $\Lambda_1 = 0$ we recover the Reissner-Norsdröm with cosmological constant Λ_0 solution of GR. The electric field equation (13) forces $\Lambda_1 < 0$

For the case B, we take $b/M = 1$; the horizon structure is similar to the case A, the differences lie on the values of Q_c and the horizon radii r_h and r_c , when they are present. Again, for $\Lambda_1 = 0$ we recover the Reissner-Norsdröm with cosmological constant Λ_0 geometry of GR. Now, the electric field equation (19) forces $\Lambda_1 > 0$.

We present the results graphically in Figs. 1, 2, and 3, displaying the most representative of them. All quantities are adimensionalized with the mass. In order to keep our analysis as general as possible, we extend the values of the parameters beyond the range that is physically expected. We let η be outside the interval $0 \leq \eta < 1$; for illustrative purposes the adimensionalized values of $|\Lambda_0|$ and $|\Lambda_1|$ used in the plots are quite large. The most interesting results come when the charge $|Q|$ is close to the critical value Q_c . Configurations in the light gray zone are stable, the dashed areas represent thin shells made of matter not satisfying WEC, and the dark gray region is non-physical (i.e. $a_0 \leq r_h$). In all figures, the top row shows for comparison the results corresponding to the solution of GR, i.e. Reissner Nordström with a cosmological constant Λ_0 . The stability regions for the selected example of the case A metric are displayed in the center row, while those of the case B in the bottom row. In Fig. 1 with $\Lambda_0 = 0$, the three spacetimes are asymptotically flat, in Fig. 2 with $\Lambda_0 < 0$ they are asymptotically anti-de Sitter, while in Fig. 3 with $\Lambda_0 > 0$ they are asymptotically de Sitter. In this last figure, the range of a_0/M displayed in the plots does not include the cosmological horizon nor the region, with unstable configurations not satisfying WEC, just before it.

From Figs. 1, 2, and 3, we can see that the value of Q_c/M and the sign of Λ_0 play a crucial role in GR as well as in both cases of UG. The main features shown in the plots are:

- In the three spacetimes considered:
 - For any $\Lambda_0 M^2$, as $|Q|/M$ increases, the minimum allowed value of a_0/M gets smaller and the stability region grows; there is a dramatic change at Q_c/M , from which an arbitrary small value of $a_0/M > 0$ is possible and very large stability region is found.
 - For $\Lambda_0 \geq 0$, if $0 \leq |Q|/M \leq Q_c/M$ the matter at the shell always satisfies WEC, but when $|Q|/M > Q_c/M$ it does not for small values of a_0/M . For $\Lambda_0 < 0$, if $0 \leq |Q|/M \leq Q_c/M$ the matter only satisfies WEC for small values of a_0/M , and if $|Q|/M > Q_c/M$ there is one zone with the matter fulfilling WEC and two zones in which do not, one for small values of a_0/M and the other one for large a_0/M .
 - For $\Lambda_0 \geq 0$, if $0 \leq |Q|/M \leq Q_c/M$ stability requires $\eta > 0$, but when $|Q|/M > Q_c/M$ any value of η is allowed if a_0/M is small enough. For $\Lambda_0 < 0$ stability with any value of η is possible, but $\eta < 0$ also requires matter not fulfilling WEC if $0 \leq |Q|/M \leq Q_c/M$.
- A comparison of the three spacetimes shows:
 - The value of Q_c/M , where an important change in behavior occurs, is smaller in UG case A than in GR and larger in UG case B than in GR.
 - For fixed values of $\Lambda_0 M^2$ and $|Q|/M$, it seems that in most scenarios the stability regions are slightly larger in the UG cases than in GR.
 - Both UG cases reduce to GR if $\Lambda_1 = 0$. In our exploration with values of Λ_1 different from those adopted in Figs. 1, 2, and 3, we have found similar features and a progressive departure from the GR results as $|\Lambda_1|$ increases.

5 Conclusions

We have presented a class of spherical spacetimes with thin shells within the theory of UG, constructed by using the junction conditions introduced in [3]. We have found the matter content for a conservative perfect fluid at the shell and the formalism for the stability of the static configurations under perturbations preserving the symmetry. For simplicity, we have taken a linearized equation of state at the shell in our stability analysis. In particular, we have applied this procedure to obtain a charged thin shell with an inner vacuum Minkowski region and an outer zone with a radial electric field. The whole spacetime does not have event horizons or singularities, but in some scenarios it has a cosmological horizon outside the shell. The energy-momentum tensor of the solution adopted for the outer part is non-conservative and we have considered two different possibilities for it, following the cases of spherically symmetric solutions found in [23]. We have compared our results with those corresponding to the GR counterpart, in which the outer zone is the Reissner-Nordström with a cosmological constant metric. We have found a qualitatively similar behavior for the matter content and for the stability of the shell in GR and in both UG geometries adopted in our construction. The value of Q_c/M , for which the main change in behavior takes place, is smaller in UG case A and larger in UG case B than in GR. For given values of $\Lambda_0 M^2$ and $|Q|/M$, the stability regions in the plane $(a_0/M, \eta)$ are generally slightly larger in the UG cases than in the GR counterpart.

Acknowledgments

This work has been supported by CONICET.

References

- [1] A. Einstein, *Sitzungsber. Preuss. Akad. Wiss. Berlin (Math. Phys.)* **1919**, 349 (1919).
- [2] W. Buchmuller and N. Dragon, *Phys. Lett. B* **207**, 292 (1988).
- [3] G. F. R. Ellis, H. van Elst, J. Murugan, and J.-P. Uzan, *Class. Quantum Grav.* **28**, 225007 (2011).
- [4] G. R. Bengochea, G. Leon, A. Perez, and D. Sudarsky, *JCAP* **11** 011 (2023).
- [5] S. Weinberg, *Rev. Mod. Phys.* **61**, 1 (1989).
- [6] S. M. Carroll, *Living Rev. Rel.* **4**, 1 (2001).
- [7] Y. Bonder, J. E. Herrera, and A. M. Rubiol, *Phys. Rev. D* **107**, 084032 (2023).
- [8] G. F. R. Ellis, *Gen. Rel. Grav.* **46**, 1619 (2014).
- [9] S. Nojiri, S. D. Odintsov, and V. K. Oikonomou, *JCAP* **05**, 046 (2016).
- [10] C. Corral, N. Cruz, and E. Gonzalez, *Phys. Rev. D* **102**, 023508 (2020).
- [11] F. X. Linares Cedeno and U. Nucamendi, *Phys. Dark Univ.* **32**, 100807 (2021).
- [12] T. Josset, A. Perez, and D. Sudarsky, *Phys. Rev. Lett.* **118**, 021102 (2017).
- [13] A. Perez and D. Sudarsky, *Phys. Rev. Lett.* **122**, 221302 (2019).

- [14] A. Perez, D. Sudarsky, and E. Wilson-Ewing, *Gen. Rel. Grav.* **53**, 7 (2021).
- [15] M. Daouda, J. C. Fabris, A. M. Oliveira, F. Smirnov, and H. E. S. Velten, *Int. J. Mod. Phys. D* **28**, 1950175 (2019).
- [16] M. A. Garcia-Aspeitia, C. Martinez-Robles, A. Hernandez-Almada, J. Magana, and V. Motta, *Phys. Rev. D* **99**, 123525 (2019).
- [17] A. O. Barvinsky, N. Kolganov, and A. Vikman, *Phys. Rev. D* **103**, 064035 (2021).
- [18] M. de Cesare and E. Wilson-Ewing, *Phys. Rev. D* **106**, 023527 (2022).
- [19] J. C. Fabris, M. H. Alvarenga, M. Hamani-Daouda, and H. Velten, *Eur. Phys. J. C* **82**, 522 (2022).
- [20] L. Amadei and A. Perez, *Phys. Rev. D* **106**, 063528 (2022).
- [21] G. Leon, *Class. Quant. Grav.* **39**, 075008 (2022).
- [22] M. P. Piccirilli and G. Leon, *Mon. Not. Roy. Astron. Soc.* **524**, 4024 (2023).
- [23] J. C. Fabris, M. H. Daouda, and H. Velten, *Universe* **9**, 515 (2023).
- [24] H. Velten and T. R. P. Carames, *Universe* **7**, 38 (2021).
- [25] T. Maudlin, E. Okon, and D. Sudarsky, *Stud. Hist. Philos. Sci. B* **69**, 67 (2020).
- [26] R. M. Wald, *Quantum Field Theory in Curved Space-Time and Black Hole Thermodynamics* (University of Chicago Press, Chicago, 1995).
- [27] J. Collins, A. Perez, D. Sudarsky, L. Urrutia, and H. Vucetich, *Phys. Rev. Lett.* **93**, 191301 (2004).
- [28] J. L. Anderson and D. Finkelstein, *Am. J. Phys.* **39** 901 (1971).
- [29] A. Perez, *Rept. Prog. Phys.* **80**, 126901 (2017).
- [30] A. Perez, *Class. Quant. Grav.* **32**, 084001 (2015).
- [31] L. Amadei, H. Liu, and A. Perez, *Front. Astron. Space Sci.* **8**, 46 (2021).
- [32] A. Perez and D. Sudarsky, *AVS Quantum Sci.* **4** 045602 (2022).
- [33] G. R. Bengochea, G. Leon, and A. Perez, *arXiv:2405.12534* (2024).
- [34] G. Darrois, *Mémoires des Sciences Mathématiques, Fascicule XXV, Chap. V* (Gauthier-Villars, Paris, 1927).
- [35] W. Israel, *Nuovo Cimento B* **44**, 1 (1966); **48**, 463(E) (1967).
- [36] P.R. Brady, J. Louko and E. Poisson, *Phys. Rev. D* **44**, 1891 (1991).
- [37] M. Ishak and K. Lake, *Phys. Rev. D* **65**, 044011 (2002).
- [38] S.M.C.V. Gonçalves, *Phys. Rev. D* **66**, 084021 (2002).
- [39] F.S.N. Lobo and P. Crawford, *Class. Quantum Gravity* **22**, 4869 (2005).

- [40] E.F. Eiroa and C. Simeone, *Phys. Rev. D* **83**, 104009 (2011).
- [41] M. Sharif and S. Iftikhar, *Astrophys. Space Sci.*, **356**, 89 (2015).
- [42] J.L. Rosa, P. Piçarra, *Phys. Rev. D* **102**, 064009 (2020).
- [43] E. Poisson and M. Visser, *Phys. Rev. D* **52**, 7318 (1995).
- [44] E.F. Eiroa and G.E. Romero, *Gen. Relativ. Gravit.* **36**, 651 (2004).
- [45] E.F. Eiroa, *Phys. Rev. D* **78**, 024018 (2008).
- [46] N. Montelongo Garcia, F.S.N. Lobo, and M. Visser, *Phys. Rev. D* **86**, 044026 (2012).
- [47] S.D. Forghani, S. Habib Mazharimousavi, and M. Halilsoy, *Eur. Phys. J. C* **78**, 469 (2018).
- [48] T. Berry, F.S.N. Lobo, A. Simpson, and M. Visser, *Phys. Rev. D* **102**, 064054 (2020).
- [49] S. Habib Mazharimousavi, M. Halilsoy, and Z. Amirabi, *Phys. Rev. D* **89**, 084003 (2014).
- [50] E.F. Eiroa, E. Rubin de Celis, and C. Simeone, *Eur. Phys. J. C* **79**, 272 (2019).
- [51] M. Visser and D.L. Wiltshire, *Class. Quantum Gravity* **21**, 1135 (2004).
- [52] N. Bilić, G.B. Tupper, and R. D. Viollier, *J. Cosmol. Astropart. Phys.* **02**, 013 (2006).
- [53] P. Martin-Moruno, N. Montelongo Garcia, F.S.N. Lobo, and M. Visser, *J. Cosmol. Astropart. Phys.* **03**, 034 (2012).
- [54] K.P. Das, U. Debnath, and S. Ray, *Phys. Dark Univ.* **46**, 101691 (2024).
- [55] F. Rahaman, M. Kalam, and S. Chakraborty, *Gen. Relativ. Gravit.* **38**, 1687 (2006).
- [56] G.A.S. Dias and J.P.S. Lemos, *Phys. Rev. D* **82**, 084023 (2010).
- [57] E.F. Eiroa and C. Simeone, *Int. J. Mod. Phys. D* **21**, 1250033 (2012).
- [58] A. Banerjee, K. Jusufi, and S. Bahamonde, *Grav. Cosmol.* **24**, 71 (2018).
- [59] E.F. Eiroa and G. Figueroa-Aguirre, *Eur. Phys. J. C* **76**, 132 (2016).
- [60] S. Habib Mazharimousavi, M. Halilsoy, and K. Kianfar, *Eur. Phys. J. Plus* **135**, 440 (2020).
- [61] E.F. Eiroa, G. Figueroa-Aguirre, and J.M.M. Senovilla, *Phys. Rev. D* **95**, 124021 (2017).
- [62] E.F. Eiroa and G. Figueroa-Aguirre, *Eur. Phys. J. C* **78**, 54 (2018).
- [63] E.F. Eiroa and G. Figueroa-Aguirre, *Eur. Phys. J. C* **79**, 171 (2019).
- [64] E.F. Eiroa and G. Figueroa-Aguirre, *Phys. Rev. D* **103**, 044011 (2021).
- [65] C. Bejarano, E.F. Eiroa, and G. Figueroa-Aguirre, *Eur. Phys. J. C* **81**, 668 (2021).
- [66] E.F. Eiroa and G. Figueroa-Aguirre, *Eur. Phys. J. Plus* **137**, 478 (2022).
- [67] F.S.N. Lobo, G.J. Olmo, E. Orazi, D. Rubiera-Garcia, and A. Rustam, *Phys. Rev. D* **102**, 104012 (2020).

- [68] J.L. Rosa, Phys. Rev. D **103**, 104069 (2021).
- [69] E.F. Eiroa, M.G. Richarte, and C. Simeone, Phys. Lett. A **373**, 1 (2008); **373**, 2399 (E) (2009).
- [70] E.F. Eiroa and C. Simeone, Phys. Rev. D **82**, 084039 (2010).
- [71] R. Wald, *General Relativity* (University of Chicago Press, Chicago, 1984).